

Controlled photon transfer between two individual nanoemitters via shared high-Q modes of a microsphere resonator

S. Götzinger,^{*} L. de S. Menezes,[†] A. Mazzei, and O. Benson[‡]

Nano-Optics, Humboldt University, Hausvogteiplatz 5-7, D-10117 Berlin, Germany

S. Kühn and V. Sandoghdar[§]

Laboratory of Physical Chemistry, ETH Zurich, CH-8093 Zurich, Switzerland

Abstract

We realize controlled cavity-mediated photon transfer between two single nanoparticles over a distance of several tens of micrometers. First, we show how a single nanoscopic emitter attached to a near-field probe can be coupled to high-Q whispering-gallery modes of a silica microsphere at will. Then we demonstrate transfer of energy between this and a second nanoparticle deposited on the sphere surface. We estimate the photon transfer efficiency to be about six orders of magnitude higher than that via free space propagation at comparable separations.

If two dipolar emitters are separated by a distance r much less than the transition wavelength λ , they can undergo strong coherent dipole-dipole coupling, leading to sub- and superradiance^{1,2}. If their transitions are broadened, dipole-dipole coupling becomes incoherent as in the case of Fluorescence Resonant Energy Transfer (FRET), where the energy from a “donor” is transferred to an “acceptor”, provided there is sufficient overlap between the former’s emission spectrum and the latter’s absorption line. The efficiency of FRET³ is proportional to $(1 + (r/r_0)^6)^{-1}$ and falls to 50% already at $r = r_0 \sim 10 \text{ nm}$. For $r > \lambda$, optical communication between the two emitters takes place via propagating photons, while the coupling drops as $1/r^2$. At a distance of $50 \text{ }\mu\text{m}$, the efficiency of one emitter absorbing a photon radiated by the other is merely 3×10^{-13} , considering a typical room temperature absorption cross section⁴ of $\sigma_A \approx 10^{-16} \text{ cm}^2$.

In order to enhance the coupling between two emitters, one could funnel the energy from one to the other by using optical elements such as lenses and waveguides. However, this process remains limited because each photon flies by the atom only once. Thus, it is interesting to exploit resonant structures to provide longer effective interaction times. In addition, resonators can influence radiative processes by modifying the density of states^{5,6}. Furthermore, if the cavity is made very small, the field per photon becomes large, resulting in a much stronger coupling between the emitter and the photon field. These effects depend on the three-dimensional locations of the donor and acceptor molecules in a decisive manner. Enhancement of the energy transfer rate in microcavities has been previously demonstrated for systems containing ensembles of molecules distributed over a volume (area) much larger than λ^3 (λ^2) in microdroplets^{7,8} or polymer microcavities⁹. However, the ideal case where two single emitters couple via photon transfer through a single mode of a high finesse microcavity remains a great experimental challenge. In this Letter we report on a major step toward this goal. We present experimental results on the controlled optical coupling and photon transfer between two individual subwavelength emitters at large distances via high-Q modes of a microresonator.

Silica microspheres melted at the end of a fiber support very high-Q Mie modes known as whispering-gallery modes (WGMs)⁶. WGMs are characterized by the radial number n and angular numbers l and m which determine their resonance frequencies and spatial intensity distributions⁶. Each mode can have polarizations TE or TM corresponding to radial magnetic and electric fields, respectively. For a sphere of radius R and refractive index N ,

an increment in l shifts the spectrum by one free spectral range $FSR = c/(2\pi RN)$. The modes with $n = 1$ and $l = |m|$ are called the “fundamental” modes and yield the most confined WGM with the largest electric field at the sphere surface. The quantities n and $l - |m| + 1$ give the number of intensity maxima along the sphere radius and perpendicular to the equator, respectively¹⁰.

We first discuss the realization of an on-command coupling between a dye-doped nanoparticle and the WGMs of a microsphere. As depicted in Fig. 1a, our strategy has been to attach the nanoparticle to the end of a fiber tip (see inset) and use a home-built Scanning Near-field Optical Microscope (SNOM) stage to manipulate the emitter in the vicinity of the microsphere surface. The recipe for the production of such probes is discussed by Kühn *et al.*¹¹ while the alignment and characterization of the microspheres and their WGMs are described in Refs^{12,13}. During all that follows, the quality factor Q of the sphere could be measured by direct spectroscopy using a narrow-band diode laser at $\lambda = 670\text{ nm}$. The fluorescent nanoparticle at the tip was excited through the fiber, and a prism was used to extract part of the particle emission that coupled to the WGMs¹⁴. Alternatively, a microscope objective (NA=0.75) allowed us to collect both the free space components of the nanoparticle fluorescence and the scattering from the sphere¹⁴.

Figure 1b shows part of the fluorescence spectrum recorded via the prism when a bead

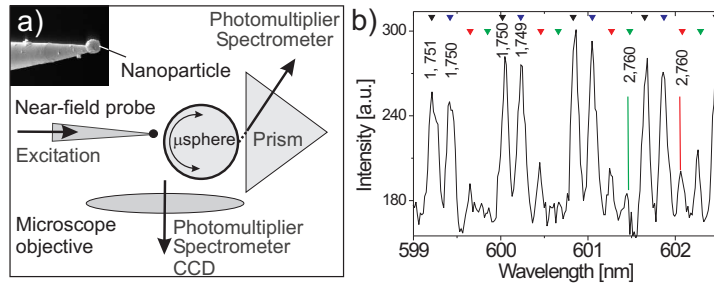


FIG. 1: a) The schematics of the experimental setup. The inset shows an SEM image of a single 500 nm bead attached to a glass tip. b) Spectrum recorded via the prism when the bead was close to the sphere’s surface. Colored triangles indicate the theoretical positions of the resonances assuming a sphere of diameter 96 μm and an index of refraction of $N=1.45724$. The fundamental modes are marked in black (TE) and blue (TM). Modes with $n = 2$ are marked in red (TE) and green (TM). The first label denotes n and the second corresponds to the l -number.

(Red Fluorescent, Molecular Probes, Inc.) of 500 nm in diameter was placed within a few nanometers of the microsphere. The spectrum shows a FSR of 0.85 nm expected for a sphere used in this measurement of $2R \approx 96 \mu m$. By using polarized detection, we identified the two dominant peaks in each FSR as TM and TE modes (see Fig. 1b). Since the small numerical aperture of our detection path via the prism was optimized for coupling to low n modes¹⁵, we attribute these resonances to $n = 1$ and the weaker ones to higher n modes.

Now, we examine the position dependence of the bead's coupling to the WGMs. To do this, we tuned the emitter's angular coordinate θ to the sphere equator¹³ and then varied its radial separation to the sphere surface using the SNOM distance stabilization and scanning machinery (see insets in Figs. 2a and b). The fluorescence emitted into the WGMs was collected through the prism coupler and detected by a photomultiplier tube. Figure 2a shows a characteristic decrease expected for the evanescent coupling between the bead and the WGMs of the microsphere. Next, we fixed the particle-sphere separation to 5 – 10 nm and scanned the bead about the equator along θ . The symbols in Fig. 2b show that the fluorescence signal detected through the prism drops quickly within 5° or equivalently $4 \mu m$ about the equator. We note that at room temperature the broad spectrum of a molecule couples to many modes of different m . However, because WGMs with higher $l - |m|$ values have larger mode volumes and therefore lower electric fields at the equator, their coupling

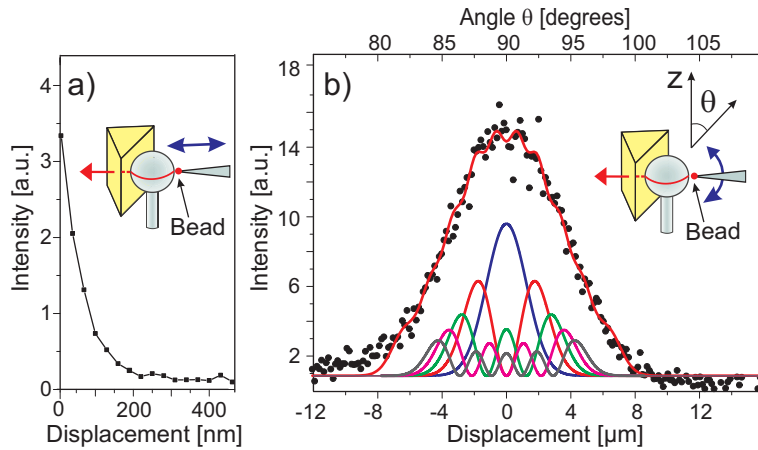


FIG. 2: Total fluorescence intensity detected through the prism coupler as a function of the sphere-bead distance (a) and the particle's lateral position (b). The thick red line in b) is a fit using the first ten WGMs. The weighted intensity distribution of only the first five WGMs is plotted for clarity.

efficiencies to both the bead fluorescence and to the prism is reduced. The red curve in Fig. 2b displays a fit to the data, accounting for the contributions of the first ten WGMs of different m . The profiles of the first five are plotted under the experimental data where the blue curve represents the fundamental mode, and the profile heights reflect the respective weighting factors in the fit procedure. The data in Fig. 2 demonstrate the local and controlled coupling of a single nanoemitter to the WGMs of a microsphere.

Next, we discuss photon transfer between a donor and an acceptor nanoparticle via the WGMs. In this experiment a sphere of $2R = 35\ \mu m$ was coated with a solution of acceptor beads (Crimson, Molecular Probes, Inc.), $200\ nm$ in diameter. After coating there were a total of less than 10 particles on the surface of the microsphere and the under-coupled Q of the fundamental mode was measured to be 3×10^7 . Then we retracted the prism to avoid losses due to output coupling and imaged the location of the acceptor beads on the microsphere using a CCD camera¹⁴. We located a single nanoparticle close to the sphere equator and centered it in the confocal detection path of the spectrometer (see Fig. 3a). A single donor bead (Red Fluorescent, Molecular Probes, Inc.) of $500\ nm$ in diameter was attached to a tip and was excited through the fiber with a laser power of $\approx 20\ \mu W$. The black and green curves in Fig. 3b show reference fluorescence spectra of the donor and acceptor beads, respectively, recorded on a cover glass. Finally, we approached the donor to the sphere and recorded the spectrum of the single acceptor bead through the microscope objective.

The red curve in Fig. 3b plots the spectrum obtained from the location of the acceptor. The fast spectral modulations provide a direct evidence of coupling to high-Q WGMs^{6,16,17,18}. Comparison of this spectrum with the black and green spectra reveals the coexistence of contributions from the donor and the acceptor fluorescence. We remark that although our confocal detection efficiently discriminates against light emitted at the donor location, it is possible for this emission to couple to the WGMs and get scattered into our collection path by the acceptor bead. To take this into account, we subtracted the donor fluorescence spectrum from the recorded (red) spectrum after normalizing their short wavelength parts. Furthermore, to rule out the possibility of direct excitation of the acceptor by the laser light, we retracted the donor from the sphere, photobleached it with an intense illumination of the excitation light and approached it again to the sphere. The signal at the acceptor position was then collected under exactly the same conditions and is shown in Fig. 3b. This

contribution is clearly negligible compared to the total emission (red curve), verifying that the acceptor fluorescence has been almost entirely pumped by the donor emission. After subtracting this small contribution, we arrive at the brown curve in Fig. 3c which coincides very well with the fluorescence spectrum of the acceptor (also shown in 3c for convenience). We note in passing that we have also checked that bleaching the acceptor bead would result in the disappearance of the longer wavelength part of the red spectrum in Fig. 3b. These measurements show, to our knowledge, the first experimental realization of photon exchange between two well-defined nanoemitters via shared high-Q modes of a microresonator. Below, we discuss the underlying physical phenomena.

Let us define the transfer efficiency η_i as the probability β_i of the donor emitting a photon into the i^{th} WGM and subsequently for this photon to get absorbed by the acceptor. Then the efficiency η_i for a photon that is emitted by the donor to be absorbed by the acceptor can be written as

$$\eta_i = \beta_i \frac{\sigma_{A,abs}}{\sigma_{A,abs} + \sigma_{D,sca} + \sigma_{D,abs} + \sigma_{i,Q}}, \quad (1)$$

where the quotient stands for the probability of a cavity photon being absorbed by the acceptor before getting lost in other channels. Note that because the emission and absorption processes are independent here (in contrast to ordinary FRET), a simple multiplication of probabilities is appropriate¹⁹. The parameter $\sigma_{A,abs}$ denotes the absorption cross section of the acceptor whereas cross sections $\sigma_{D,sca}$ and $\sigma_{D,abs}$ quantify losses out of the mode due to scattering and absorption of a photon by the donor. Finally, $\sigma_{i,Q}$ is a cross section signifying all losses associated with the measured Q of the microsphere, including those caused by scattering from the acceptor. A small mode volume is therefore, important for the enhanced emission rate of photons from the donor into the sphere and enters the quantity β_i . Furthermore, the high Q and hence small $\sigma_{i,Q}$ result in the enhanced absorption probability of photons by the acceptor. Both effects are absent if light is transferred merely by a waveguide or optical fiber.

The cross sections used in Eq. (1) are, strictly speaking, defined for evanescent illumination and different from those commonly quoted for plane wave excitation. The deviation between the two quantities can be notable, but it has been shown that it remains well within a factor of 3 even for strongly scattering silver particles of diameter 200 nm at plasmon resonance²⁰. Thus, in our case it is appropriate to use the conventional values of the cross sections for obtaining an order of magnitude estimate. The absorption cross section

of the acceptor particle can be taken as $\sigma_{A,abs} \approx 10^{-11} \text{ cm}^2$, assuming $\sigma_{abs} \approx 10^{-16} \text{ cm}^2$ per molecule⁴ and 10^5 molecules per particle. Since due to the Stokes shift of molecular fluorescence the donor does not absorb its own emission very efficiently, we can neglect $\sigma_{D,abs}$. In addition, we obtain $\sigma_Q = 2 \times 10^{-12} \text{ cm}^2$ for a fundamental mode based on $Q = 3 \times 10^7$. Since in our experiment the measured Q remained unchanged as the tip approached the microsphere, we conclude that $\sigma_{D,sca}$ was negligible compared to σ_Q ²¹. We find, therefore, that for a fundamental mode, the quotient in Eq. (1) is about 10^{-4} considering a single molecule acceptor.

In the weak coupling regime, the spontaneous emission rate Γ can be written as $\Gamma = \frac{2\pi}{\hbar^2} |\langle e | \mathbf{E} \cdot \mathbf{D} | g \rangle|^2 \rho(\omega)$ where \mathbf{E} is the fluctuating vacuum field at the location of the emitter, \mathbf{D} is the dipole operator associated with the optical transition at hand, and ρ is the density of photon states. Hence, the strength of emission into different WGMs and consequently β_i ,

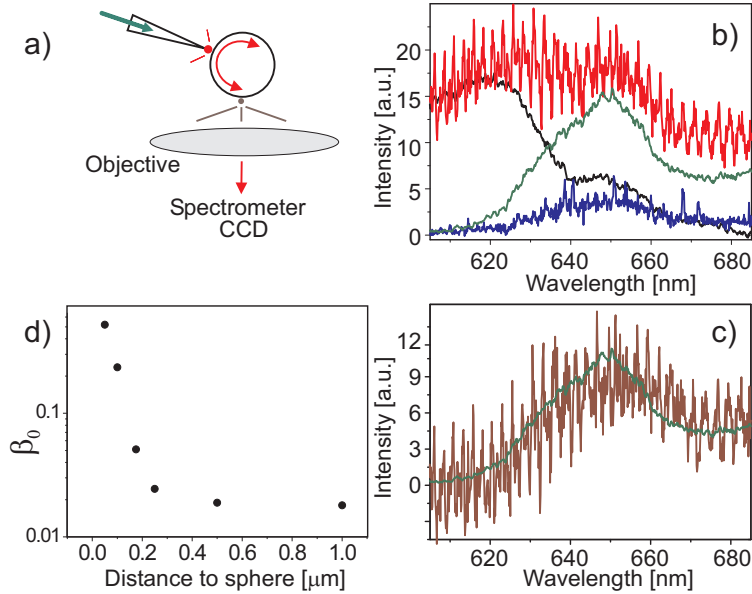


FIG. 3: a) Scheme of the cavity-mediated photon transfer measurement. b) The black and the green curves display the reference fluorescence spectra of the naked donor and the acceptor beads, respectively. The red curve shows the recorded spectrum when a donor is brought close to the sphere's surface. The blue curve shows the same measurement after bleaching of the donor. c) The brown curve plots the net emission spectrum of the acceptor as a result of photon transfer. The green curve shows the normalized spectrum of a free acceptor from (b) for comparison. d) Calculated dependence of β_0 on emitter's separation from the microsphere.

are proportional to the projection of each mode's field intensity $|E_i|^2$ at the sphere surface onto the dipolar axis. In what follows we calculate β_i for the fundamental mode and use its scaling with $|E_i|^2$ to evaluate the contribution of other WGMs to the energy transfer process.

Since the seminal work of Purcell, it is known that spontaneous emission of a narrow-band dipole is enhanced when it is coupled to a resonator mode⁵. This enhancement is reduced if the linewidth of the dipole is broadened to Γ_b , greater than the cavity linewidth Γ_{cav} , as is the case for $\Gamma_{cav} = 6 \times 10^{-5} \text{ nm}$ and $\Gamma_b \approx 20 \text{ nm}$ in our experiment. The ratio β , of the emission into the cavity mode to the total emitted power is thus, given by $\beta \approx \beta_0(\Gamma_{cav}/\Gamma_b)^{22}$ whereby β_0 represents the fraction for a narrow-band emitter. Note that since $\beta_0 \propto Q$, in this case β becomes independent of Q . To calculate β_0 for a fundamental mode, we calculated the power radiated into this mode²³ by approximating the emission of a randomly oriented dipole by a spherical wave and calculating its overlap with the mode²⁴. The finite Q of the sphere was accounted for by using a complex N ²⁵. Figure 3d shows the result as a function of the distance between the emitter and the sphere's surface. We find that $\beta_0 = 0.5$ at a distance of 50 nm from the sphere surface, leading to $\beta_i = 1.5 \times 10^{-6}$.

For other WGMs, higher n and $l - |m|$ result in an increase of the mode volume and lower $|E_i|^2$ values. By computing the mode functions of the various WGMs, we have determined $|E_i|^2$ on the sphere surface normalized to its value for the fundamental mode. Furthermore, by calculating the diffraction limited Q for various n ²⁶, we have determined the dependence of the quotient in Eq. (1) on this parameter. Combining these results we find that for each l the contribution to $\eta = \sum \eta_i$ of modes with $n > 10$ drops by an order of magnitude. We also find that the first 40 modes with different $l - |m|$ values account for half the contribution of all modes. Considering that the fluorescence spectrum of a bead spans about 20 FSRs ($FSR = 2.3 \text{ nm}$ for $2R = 35 \text{ }\mu\text{m}$) and taking into account both TE and TM modes, we conclude that η is about $10 \times 40 \times 20 \times 2 \approx 2 \times 10^4$ times larger than that of a single fundamental mode. Putting all the above-mentioned information together, we find that $\eta \approx (1.5 \times 10^{-6}) \times 10^{-4} \times 2 \times 10^4 \approx 10^{-6}$ for a single molecule acceptor which is more than six orders of magnitude larger than the free-space rate for absorbing a photon emitted at a distance of about 35 micrometers.

We have demonstrated that the application of scanning probe techniques allows one to achieve an on-command and efficient evanescent coupling between a nanoscopic emitter and

a WGM resonator. In the current system we have coupled the broad-band emission of dye molecules to a large number of resonator modes in a dissipative energy transfer process. Under these conditions, the role of the high cavity Q in the enhancement of spontaneous emission has been negligible. Instead, the importance of the high Q has been to circulate each photon a large number of times, increasing its chance of interaction with the acceptor. However, at low temperatures emitter transitions as narrow as a few tens of MHz can be achieved, enhancing the photon transfer efficiency between single emitters by an additional five orders of magnitude. Furthermore, one could get around the inhomogeneous distribution of resonance frequencies by local application of electric fields² and use our experimental arrangement to achieve controlled coherent coupling of individual quantum emitters mediated by a high- Q microcavity²⁷. Indeed, cryogenic efforts have already demonstrated the coupling of single molecules to WGMs²⁸ and their manipulation at the end of a tip²⁹.

We acknowledge funding from the DFG (SP113) and the Swiss National Foundation. L. de S. Menezes acknowledges the fellowship from the Alexander von Humboldt Stiftung. A. Mazzei acknowledges financial support of NaFöG, Berlin.

* Present address: Edward L. Ginzton Laboratory, Stanford University, Stanford, CA 94305, USA

† Permanent address: Depto. de Física, Universidade Federal de Pernambuco, 50670-901 Recife-PE, Brazil.

‡ Electronic address: oliver.benson@physik.hu-berlin.de

§ Electronic address: vahid.sandoghdar@ethz.ch

¹ R. H. Dicke, Phys. Rev. **93**, 99 (1954).

² C. Hettich, et al., Science **298**, 385 (2002).

³ T. Förster in *Modern Quantum Chemistry*, Vol. III (O. Sinanoglu, ed.) 93-137, Academic Press, N.Y. (1965).

⁴ F. P. Schäfer, *Dye Lasers*, Springer Verlag, Berlin (1990).

⁵ P. Berman, Ed., *Cavity Quantum Electrodynamics*, Academic Press, London, (1994).

⁶ R. K. Chang and A. J. Campillo, *Optical Processes in Microcavities*, World Scientific, Singapore (1996).

⁷ L. Folan, S. Arnold, and S. Druger, Chem. Phys. Lett. **118**, 322 (1985).

- ⁸ S. Arnold, S. Holler, and S. D. Druger, J. Chem. Phys. **104**, 7741 (1996).
- ⁹ M. Hopmeier, W. Guss, M. Deussen, E. O. Gobel, and R. F. Mahrt, Phys. Rev. Lett **82**, 4118 (1999).
- ¹⁰ J. C. Knight, et al., Opt. Lett. **20**, 1515 (1995).
- ¹¹ S. Kühn, C. Hettich, C. Schmitt, J.- Ph. Poizat, and V. Sandoghdar, J. Microscopy **202**, 2 (2001).
- ¹² S. Götzinger, O. Benson, and V. Sandoghdar, Appl. Phys. B **73**, 825 (2001).
- ¹³ A. Mazzei, S. Götzinger, L. de S. Menezes, V. Sandoghdar, and O. Benson, Opt. Comm., **250**, 428 (2005).
- ¹⁴ S. Götzinger, et al., J. Opt. B **6**, 154 (2004).
- ¹⁵ M.L. Gorodetsky and V.S. Ilchenko, Opt. Comm. **113**, 133 (1994).
- ¹⁶ J. D. Eversole, H.-B. Lin , and A. J. Campillo, Appl. Opt. **31**, 1982 (1992).
- ¹⁷ X. D. Fan, P. Palinginis, S. Lacey, H. L. Wang, and M. C. Lonergan, Opt. Lett. **25**, 1600 (2000).
- ¹⁸ H. Yukawa, S. Arnold, and K. Miyano, Phys. Rev. A **60**, 2491 (1999).
- ¹⁹ P. T. Leung and K. Young, J. Chem. Phys. **89**, 2894 (1988).
- ²⁰ M. Quinten, A. Pack, and R. Wannemacher, Appl. Phys. B. **68**, 87 (1999).
- ²¹ S. Götzinger, O. Benson, and V. Sandoghdar, Opt. Lett. **27**, 80 (2002).
- ²² K. Ujihara in *Spontaneous Emission and Laser Oscillation in Microcavities*, H. Yokoyama, K. Ujihara eds., CRC Press (1995).
- ²³ V. V. Klimov, M. Ducloy, and V. S. Letokhov, J. Mod. Opt. **43**, 2251 (1996).
- ²⁴ J. P. Barton, D. R. Alexander, and S. A. Schaub, J. Appl. Phys. **64**, 1632 (1988).
- ²⁵ H. T. Dung, L. Knöll, and D-G. Welsch, Phys. Rev. A **64**, 013804 (2001).
- ²⁶ V. V. Datsyuk, Appl. Phys. B. **54**, 184 (1992).
- ²⁷ A. Imamoglu, et. al., Phys. Rev. Lett. **83**, 4204 (1999).
- ²⁸ D. J. Norris, M. Kuwata-Gonokami, and W. E. Moerner, Appl. Phys. Lett. **71**, 297 (1997).
- ²⁹ J. Michaelis, C. Hettich, J. Mlynek, and V. Sandoghdar, Nature **405**, 325 (2000).